PARABOLA III: a sphere-scanning radiometer for field determination of surface anisotropic reflectance functions

Carol J. Bruegge, Mark C. Helmlinger, James E. Conel, Barbara J. Gaitley, Wedad A. Abdou

Jet Propulsion Laboratory, California Institute of Technology, Pasadena, CA 91109

ABSTRACT

The Portable Apparatus for Rapid Acquisition of Bidirectional Observation of the Land and Atmosphere III (PARABOLA III) is a sphere-scanning radiometer.The original PARABOLA was built to study the relationship between surface morphology and reflected radiation properties. Follow-on work led to the design of an improved radiometer, the PARABOLA III. This in-situ sensor will be used to validate surface reflectances at angles measured by the Multi-angle Imaging SpectroRadiometer (MISR), a global imager flown on the Earth Observing System (EOS)-Terra orbital spacecraft. Derived PARABOLA III data products include the surface bidirectional reflectance factor, and sky and surface radiances for the upward and downward viewing hemispheres. This paper describes the design, calibration, and operation of the JPL PARABOLA III.

1. INTRODUCTION

With the advent of a new generation of calibrated, global multi-angle instruments, a rich data set is now available to apply to traditional remote sensing objectives, as well as to the study of Earth's climate and mechanisms which may lead to climate change. One such orbital sensor is the Multi-angle Imaging SpectroRadiometer (MISR), launched December 18, 1999 on-board the Earth Observing System (EOS)-Terra spacecraft (Diner, et. al. 1998). MISR views the surface at nine angles simultaneously (nadir, $\pm26.1°$, $\pm45.6°$, $\pm60.0°$, and $\pm70.5°$) and in four spectral filter bandpasses, 446, 558, 672, and 866 nm. The azimuth of MISR's ground track, following an inclination 98.3°, depends on latitude. Observations cover a large range of scattering angles with respect to the sun-surface-sensor. Studies have shown that the amount of radiation scattered back towards space can be derived from MISR's discrete-view samples to a high degree of accuracy [Lucht, 1998]. Additionally, MISR is testing new approaches to the retrieval of aerosol abundance and type, and land and cloud morphology [Martonchik, 1998].

Multi-angle viewing sensors, such as MISR, can be used to derive the surface Hemispherical Direction Reflectance Factor (HDRF) and the Bidirectional Reflectance Factor (BRF) [Martonchik, 1994]. The HDRF refers to the reflectance properties of the surface due to the atmosphere and illumination conditions present during a particular measurement campaign. Conversely, the BRF is a fundamental property of the surface alone, is independent of the diffuse sky light contributions, and describes the redistribution of light at the surface due to an incident collimated beam. Although not as straightforward to compute, the BRF is the preferred surface descriptor. It is used as an input to radiative transfer propagation studies linking the surface and on-orbital boundary layers.

MISR measurements are also used to retrieve the fractional photosynthetic active radiation (FPAR). This biophysical parameter is defined in terms of the albedos under direct illumination (the directional-hemispherical reflectance, DHR) plus canopy model dependent functions. Ordinary measurements of albedo using albedometers lead to inappropriate approximations of this parameter, while the retrieved BRF does allow for an accurate representation of FPAR. Additionally, other key variables that describe land characteristics, such as the normalized difference vegetation index (NDVI), can be best made insensitive to atmospheric illumination conditions, and diurnal illumination differences, through use of multi-angle measurements.

One significant program to utilize in-situ, multi-angle data sets in the investigation of land cover/ radiation interactions was begun over a decade ago (Deering and Leone, 1986). The Portable Apparatus for Rapid Acquisition of Bidirectional Observation of the Land and Atmosphere (PARABOLA) instrument was commissioned to facilitate this work. (See http://parabola-web.gsfc.nasa.gov/parabola/source). This instrument samples radiance originating from the upwelling surface direction, as well as the downwelling sky direction. Full-sphere coverage is obtained in discrete field-of-view samples. One specification was to build a sensor that could acquire multi-angle measurements in a sufficiently small time interval such that the effects of changing sun, sky, and vegetation dynamics could be minimized. The original instrument consists of three spectral bands (650-670, 810-840, and 1620-1690 nm), has a 15° field-of-view, and sampled the complete 4π sterradians in 11 seconds. The PARABOLA III was designed to extend the wavelength coverage and to decrease the field-of-view. Two such PARABOLA III instruments

currently exist: one owned by the NASA/ Goddard Space Flight Center (GSFC), and the other by the Jet Propulsion Laboratory (JPL). The latter is dedicated to the task of providing MISR validation data products. Information on field campaigns which have involved this PARABOLA can be found at http://www-misr.jpl.nasa.gov/mission/vinstrum.html. We give a description of this instrument and its characteristics in this paper; the derivation of surface reflectances using this instrument is provided in a companion paper (Abdou et al., 2000).

2. INSTRUMENT DESCRIPTION

PARABOLA III was designed and built by Sensit Technologies, Inc. (Hereafter we use the terms "PARABOLA" and "PARABOLA III" interchangeably to refer to the JPL owned PARABOLA III instrument). As shown in Figure 1, it consists of two separate sensor heads mounted at opposite ends of a center-suspended horizontal scanning beam that rotates continuously through 360° in azimuth. Each sensor head has four independent radiometers which, in turn, scan synchronously from zenith to nadir. The instrument is suited for field conditions, as the azimuth and the zenith drives are the only moving parts. The motions about the vertical and horizontal axes generate a stepwise pattern in elevation angle increments of 5° and a stepwise pattern in azimuth angle in increments of 5°. An entire scan of both sky and ground hemispheres generates 2664 samples (37 x 72) in about 3.3 minutes. This includes downloading the angle position data and instrument responses to memory. Figures 2a and 2b show the field-of-view (FOV) projections onto the sky hemisphere, and ground projections, respectively. The samples are tangent at the horizon. These circular FOVs progress towards increasing overlap as the zenith is approached, leading to a varying degree of oversampling. For the ground hemisphere, the pattern is that of elliptical FOVs, increasing in size with increasing view angle from nadir. The ground pattern leads to oversampling at nadir and some undersampling at the horizon. The size of these

samples is shown in the figure compared to a metric ruler, and represent the projected FOV of PARABOLA when mounted 2 m above the ground.

Figure 1. The PARABOLA III scanning radiometer. Shown are the two sensor
heads, eight spectrally-filtered radiometers, a reflectance standard, power supply,
Zip drive housing, and guy-wired stand.

Each radiometer consists of a telescope, with a unique filter, and sun shade. The eight spectral channels are at wavelengths of 444, 551, 581, 650, 860, 944, 1028, and 1650 nm. Four of these (444, 551, 650, and 860 nm) provide data within MISR-like spectral bands. Additionally, one channel exists for the characterization of water vapor (944 nm), and two for characterization of aerosol optical depth at longer wavelengths (1028 and 1650 nm). The latter channel is also used

for vegetation studies. Finally, a broad-band channel (400-700 nm, centered at 581 nm) provides measurement of photosynthetic active solar radiation (PAR).

a. sky view
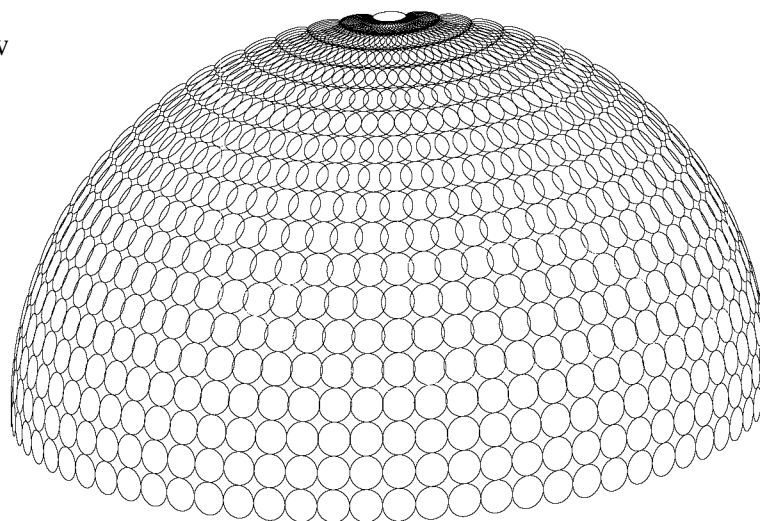
b. ground projection of field-of-view samples
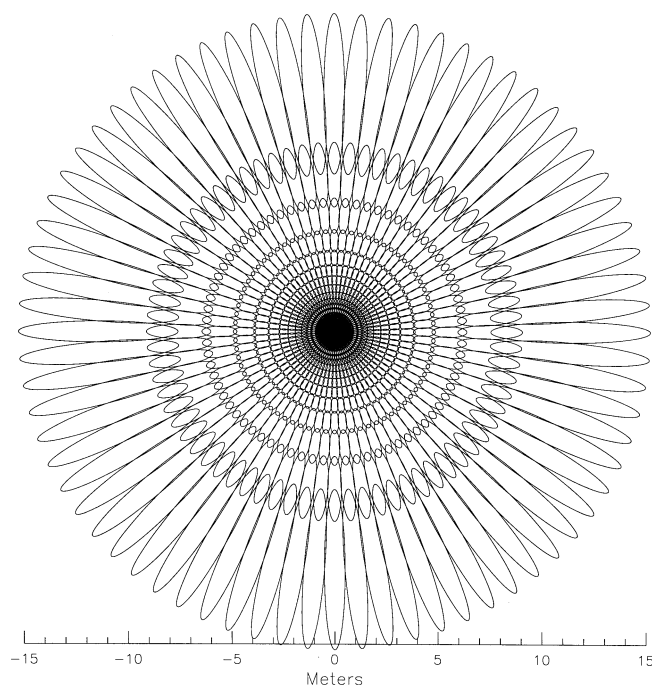
Figure 2. The field-of-view projection onto the sky hemisphere, and ground projections, are shown respectively in (a) and (b).

A schematic of the telescope layout is given in Figure 3. The geometric fields of view of each channel are determined by a field stop located in front of the detector plane, and a front entrance aperture located behind the filter. Although the filter is located external to this aperture, it does not

restrict or define the field-of-view. This arrangement produces a full-field-of-view (apex at detector center) of 5°, and an annular surrounding zone of partial illumination extending out to full angle of 8°. Three baffles arranged along the telescope tube help to reduce stray light.
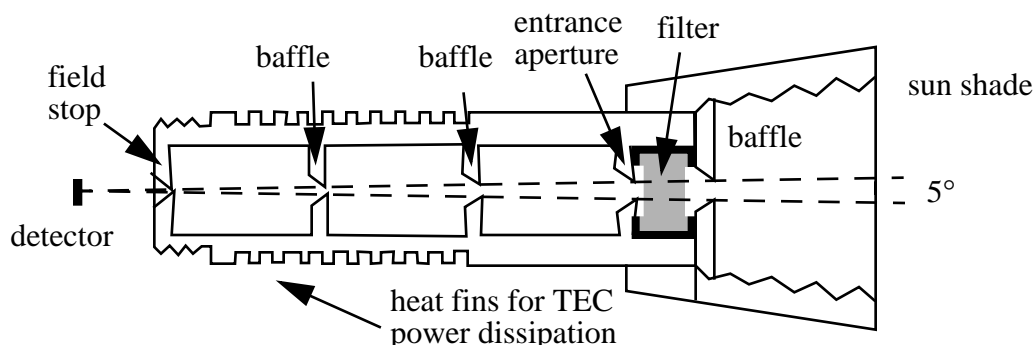
Figure 3. Telescope layout, showing the detector plane, field-defining apertures, baffles, and filter locations.

Three of the four radiometers within each head use of silicon (Si) detectors; the fourth detector is made of germanium (Ge), for 1028 and 1650 nm detection. Each focal plane is manufactured as a unit, evacuated, and hermetically sealed to allow for detector cooling and to provide protection from harsh environmental elements. The focal plane design is depicted in Figure 4. A cooled transimpediance operational amplifier (op-amp) converts the detector current to a voltage. An external metal-film, thermally insensitive, precision resistor is selected to provide the desired gain. A large dynamic range is available, in that a 20 bit analog-to-digital (A/D) converter is used. A separate A/D exists for each of the eight spectral channels, and two 12 bit A/Ds exist for engineering data. To reduce noise, the radiometer A/D converters are mounted directly behind the detector packages. These are operated in parallel, preventing a data bottle-neck which would otherwise ensue using a serial operation.
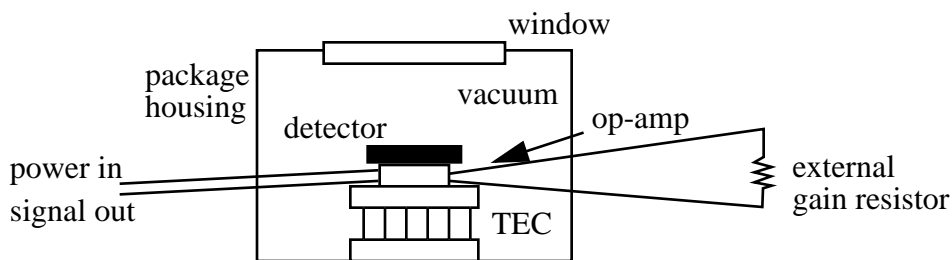
Figure 4. Focal plane layout showing components within hermetic seal.

The detector and op-amp are mounted to the cold side of a thermo-electric cooler (TEC). The temperature is controlled to -10° C. This reduces detector and amplifier noise, and additionally maintains a constant radiometric response, independent of external environmental temperatures. Frost build-up is not a problem because of the sealed package. The Ge detector in each head is monitored with a thermistor, temperatures are recorded in the data stream, and active control is provided by varying the current to each of the four TEC's in the head, which are connected in series.

Operation of the instrument is controlled by an imbedded 386/ 50 MHz microprocessor. The driving code is stored onto flash memory chips, emulating a hard disk and providing non-volatile memory. This solid-state device is desirable for field conditions, and requires no battery support for data retention. The control code is written in DOS-based Turbo Pascal. Repetitive tasks, such as the control of the zenith motors, are delegated to a second, stamp-type, microprocessor. Rapid collection of data has been enabled by other modifications which remove simple repetitive tasks from the main microprocessor.

PARABOLA III contains a two axes electronic compass and level such that yaw, roll, and pitch can be determined. The reporting of these to the data stream make PARABOLA suited for boat or aerial tram operation. The overall orientation of the head is believed known to ± 1°. Knowledge of the instrument motion during data acquisition could allow for a correction of these effects in the analysis, if needed. (To date we have relied upon PARABOLA remaining stationary over a given target throughout the duration of the day). An external camera trigger can be programmed to record sky and surface conditions at any time during a scan. Another feature of interest is the geometric audible tones which play during instrument operation. These are diagnostic, and indicate the beginning and ending of an operational sequence. An interruption in this ordered set of aural cues quickly alerts an operator to instrument malfunction. The position of the Sun in the sky, needed for data interpretation and to record the angle of incidence, is accurately determined from the solar ephemeris, given the geographic coordinates.

For PARABOLA field operation a field researcher first looks for a flat region, homogeneous over 30 m spatial scales. As shown in Figure 1, the instrument is mounted on a pole, and stabilized using three guy wires. Bottom mounted connectors allow all cables to be run down the center axis,

through the center of the U-shaped pole. For ultimate portability, power to the instrument is obtained from a set of ten solar panels which charge a 60 Amp-hr, 12 V sealed battery. This is stepped up to the 110 V needed to traverse the distance from the solar farm to the instrument. Light, 16 gauge, 30 m extension cords are used, as a mere 50 W of power is required. The power must be stepped down again to the 5, 12, and 24 V inputs at the destination. The nadir most 10 to 15 pixels are contaminated due to the presence of the power supply and 100 MB Zip drive housing. This gives an ideal platform for a 10" square Spectralon panel, used in the algorithm to transfer the output digital numbers, obtained while viewing the Earth target, into a reflectance [Bruegge, 2000].

A laptop computer is brought into the field to initialize the instrument. The clock is first set to universal time (UT). This is needed as the microprocessor loses 3 seconds per day. The zenith drive is next calibrated by manually positioning the heads to the zenith and nadir directions respectively, informing the instrument of the appropriate settings. After the directory structures and filename prefixes have been created, continuous data acquisition begins, with data written to the Zip cartridge. Several full-day collections can be stored on the Zip cartridge. During the day, the field engineer makes periodic inspections of the instrument, including listening for deviations from its atonal "song". Care is taken to minimize any disturbance to the surface beneath and around PARABOLA.

3. INSTRUMENT CHARACTERIZATION AND CALIBRATION

3.1 Gain determination

As part of a one-time instrument check-out, the JPL PARABOLA was set to track the sun throughout a morning, without head rotation. A Langley analysis was then performed on these data. That is, a logarithmic form of Beer's law, $\ln (DN)=(-\tau m) + \ln (DN_o/d^2)$, was assumed, and an extrapolation to an airmass, m, of zero was used to determine DN_o, the digital number the instrument would produce at the top of atmosphere. (Here DN is the instrument output digital number with the original gain resistor, τ the atmospheric optical depth, and d^2 the Earth-Sun distance on the day of observation). This analysis was done independently for each channel. In the final step a gain resistor, R, was selected such that A/D input voltage saturation was set to a value of 20% above the response to the exo-atmospheric sun:

$$R_{new} = \frac{(2^{20})R_{old}}{1.2DN_o} \tag{1}$$

3.2 Field-of-view verification

In order to verify the fields-of-view of each of the eight PARABOLA radiometers, a special test was conducted. PARABOLA was mounted to a custom tracking mount, with the capability for providing fine elevation and azimuth adjustments every 20 seconds. During the afternoon, the instrument was set up so that the sun was centered in each radiometer's field-of-view and allowed to track the sun for some period of time. Readings of all radiometers were recorded roughly every 30 seconds. Following this the tracking was shut off, and the sun slowly moved outside the angular response range of the sensor. Figure 5 shows the results of this experiment, verifying the 5° field-of-view design. An ephemeris was used to determine the sun's position as it traversed outside the field-of-view.
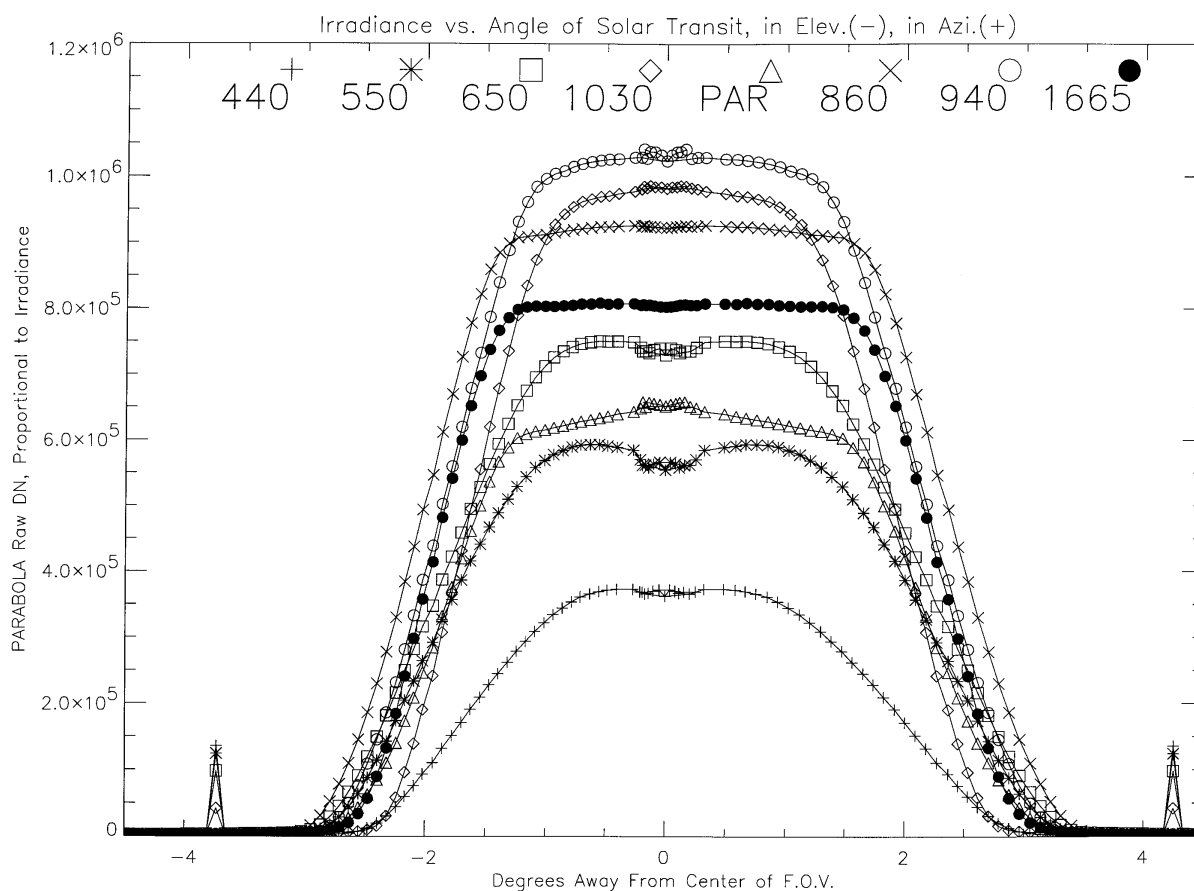
Figure 5. Field-of-view determination, using the sun as a source.

3.3 Spectral calibration

A primary objective of the MISR validation program is to intercompare surface reflectance observations with those retrieved from orbit. Ideally these comparisons would be done using instruments with identical spectral band shapes. As this is not possible, a correction for spectral differences is required. Irrespective of this objective, we desire to report PARABOLA retrievals specific to the spectral channels for this instrument. The most complete descriptor of a spectral channel is the relative instrument response as a function of wavelength. We require this response to be measured for the complete optical system including the filter, focal plane window, and detector. For practical purposes we derive the center wavelength and bandwidth descriptors from the response profile.

Spectral calibration data were acquired October 6, 1998 using a double pass monochromator. The response functions for all channels were determined in the laboratory by illuminating the entrance aperture of each radiometer with a collimated beam of light. The source was a quartz-halogen incandescent lamp, driven from a constant current source. The system is designed to characterize instrument response in the 250 - 3500 nm range. For the 250 to 1100 nm region the monochromator output is monitored by a silicon photodetector; otherwise a germanium photodetector is used. These monitoring signals were used to normalize the actual monochromator output signal such that the response to an effective constant source with wavelength is obtained. Because the monochromator output is weak as compared to the saturation level of PARABOLA, a chopped source/lock-in detection system was used, operating at a chopping frequency of 200 Hz. The electronic output of PARABOLA was detected by picking off the analog signal at the input to the A/D converter for each band. The resulting spectral response functions are shown in Figure 6.
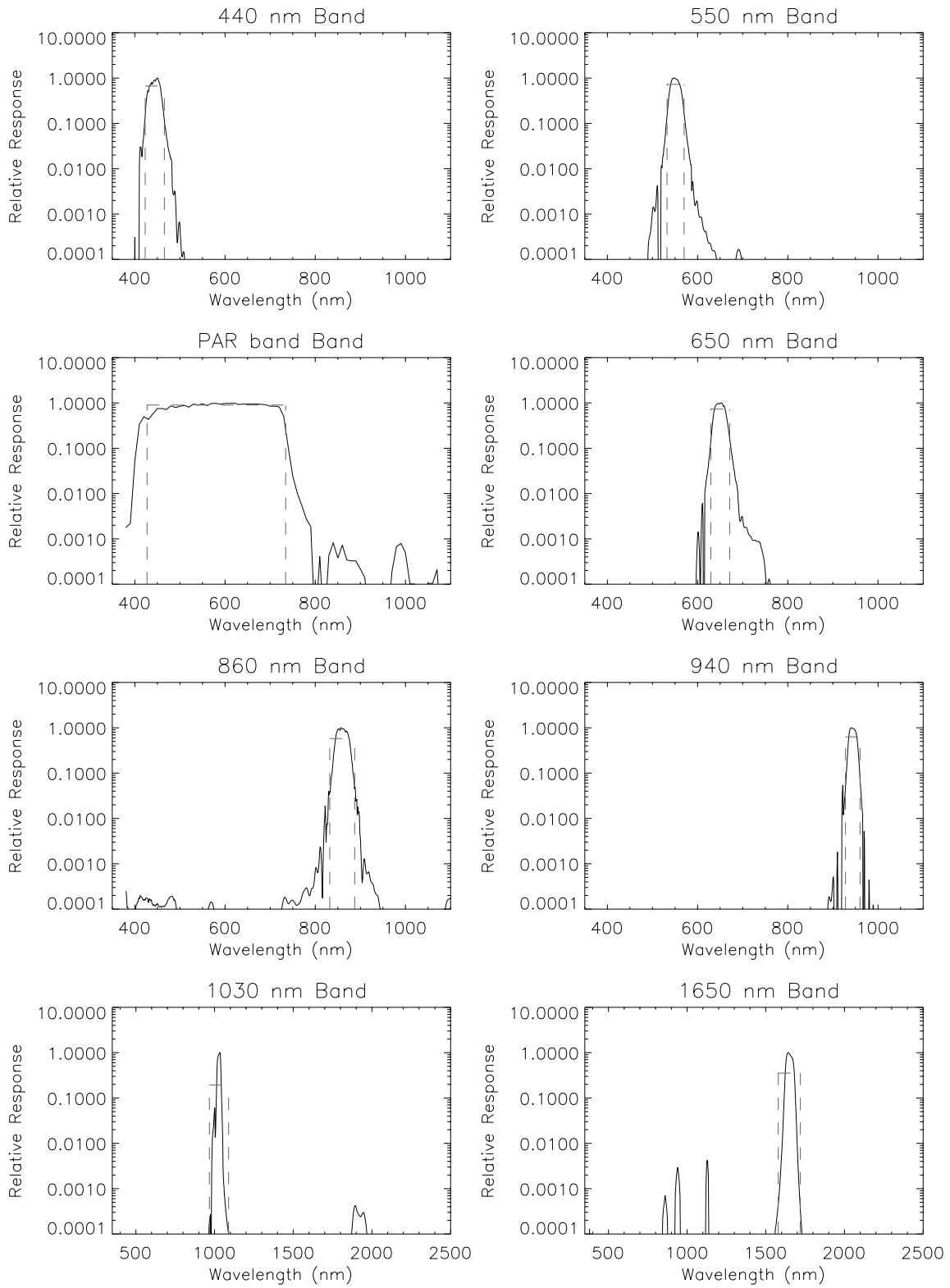
Figure 6. Spectral response functions for the eight PARABOLA III channels, multiplied by the exo-atmospheric solar irradiance. The dashed lines show the equivalent square band response. Note there is a wavelength scale change for the last two channels.

The retrieval of center wavelength and bandwidth is accomplished using the same algorithm as used for MISR data reductions [Bruegge, et al., 1998b]. We make the assumption that many radiance measurements will have the same relative spectral distribution as the solar spectrum. In our moments analysis, therefore, we weight the camera response function by the exo-atmospheric solar irradiance. The as-built PARABOLA III wavelengths that are quoted are those descriptive of the total-band response region, weighted by the solar spectrum:

$$\lambda_{m, solar} = (\int E_{o\lambda} R_{\lambda} \lambda^2 d\lambda) / (\int E_{o\lambda} R_{\lambda} \lambda d\lambda) \qquad (2)$$

$$\sigma^2 = (\int E_{o\lambda} R_{\lambda} \lambda^3 d\lambda / \int E_{o\lambda} R_{\lambda} \lambda d\lambda) - (\lambda_{m, solar})^2 \qquad (3)$$

$$\lambda_{u, l} = \lambda_{m, solar} \pm (\sqrt{3} \cdot \sigma) \qquad (4)$$

$$\Delta \lambda_{m, solar} = 2\sqrt{3} \cdot \sigma \qquad (5)$$

Here R_{λ} is the sensor response to incident photons and $R_{\lambda} \lambda$ is proportional to the incident radiance. The subscript m denotes moments analysis; and u, and l the equivalent square band upper and lower wavelength limits, respectively. The exo-atmospheric solar irradiance, $E_{o\lambda}$, model used by MISR is one recommended by the EOS calibration panel. The data are published by the World Climate Research Programme [Wehrli, 1985]. Values are reported at 1 astronomical unit (AU).

The results of the spectral analysis are given in Table 1 below. These are reported for a moments analysis done over both the solar-weighted total, and in-band regions. The in-, out-band boundary is defined at the wavelength where the response falls to 1% below peak. It is shown that there are little differences between these parameters, in that PARABOLA has high out-of-band rejection. The out-of-band response is tabulated in the last column, computed from the out-of-band

area under the $E_{o\lambda}$ R_λ λ curve, ratioed to the total area. Only the 1028 nm band exhibits an undesirable out-of-band response with a value of 3%.

Table 1. PARABOLA spectral parameters

Total-band		In-band		
center wavelength $\lambda_{m,c}$ (nm)	bandwidth $\Delta\lambda_{m,c}$ (nm)	center wavelength $\lambda_{m,c}^{in-band}$ (nm)	bandwidth $\Delta\lambda_{m,c}^{in-band}$ (nm)	out-of-band response, %
444.3	42.4	444.3	38.3	0.62
551.2	37.7	551.1	35.5	0.35
580.7 (PAR)	307.2	580.7	307.2	0.10
650.3	41.9	650.0	38.9	0.43
859.7	55.2	860.0	39.9	0.35
944.0	32.2	944.2	25.0	0.65
1028.4	121.9	1027.8	41.2	3.03
1649.6	140.8	1650.9	88.1	0.44

Table 2 provides a comparison of spectral parameters to the MISR standardized spectral response functions. (The term "standardized" refers to an average value for all field positions of all nine line arrays associated with the instrument, for a common spectral band). MISR passbands are gaussian in shape, to facilitate the depolarization design. This is one reason for the larger MISR bandwidths and out-of-band response. In addition, scattering within the filter is believed to increase the out-of-band energy, over that predicted from the theoretical model [Korechoff, 1996]. The MISR center wavelengths most typically reported in the literature are those computed over the in-band response. This is adopted as many derived geophysical data products begin with radiances that have been corrected for out-of-band response [Chrien, 1996]. For PARABOLA, we will quote the total band-center wavelengths. No out-of-band correction is presently performed in deriving PARABOLA data products.

Table 2. MISR spectral parameters

Total-band		In-band		
center wavelength $\lambda_{m,c}$ (nm)	bandwidth $\Delta\lambda_{m,c}$ (nm)	center wavelength $\lambda_{m,c}^{in-band}$ (nm)	bandwidth $\Delta\lambda_{m,c}^{in-band}$ (nm)	out-of-band response, %
447.5	69.5	446.3	40.9	1
557.8	74.5	557.5	27.2	2-3
669.5	91.9	671.8	20.4	2
857.8	184.2	866.5	38.6	0.8-2

4. RADIOMETRIC CALIBRATION

In making use of PARABOLA to derive surface BRF functions (and thereby validate MISR retrievals), it is sufficient to scale the instrument output using a reflectance standard (Abdou, 2000; Bruegge, 2000). However, for completeness a radiometric calibration was conducted, with the goal of obtaining a 10% uncertainty. During radiometric calibration the relationship between an incident radiance field and instrument output is established. The illumination is achieved using an ideal target that emits or reflects unpolarized light, is spatially and angularly uniform, and lacks spectral features such as absorption lines. For this determination PARABOLA made use of a large integrating sphere. The sphere is 1.6 m (65") in diameter, has a 76x23 cm (30x9") exit port, and a 30 cm (12") external satellite sphere with variable aperture. It is sequenced through a number of lamp-on settings, allowing digital data to be collected at radiometric levels evenly spaced within the dynamic range of each spectral channel. The sphere was also used in the preflight calibration of MISR; its size and the calibration procedures were primarily designed to support MISR testing. Difference between MISR and PARABOLA include dynamic range and the location of specific spectral bands. Both MISR and PARABOLA measure light in the range expected for diffuse skylight and surface reflected radiance; only PARABOLA is designed to cover six orders of magnitude of illumination, thus allowing direct observations of the solar disk. The PARABOLA calibration discussed in this section describes the radiometric response in that portion of the sensor which measures surface reflected radiances (the lower 10 bits). Specifically, the range of

equivalent reflectances for which this calibration is valid is roughly between zero and one. Here equivalent reflectance, ρ_{eq}, is a normalized measure of the energy directed towards the camera:

$$\rho_{eq}=L_\lambda \, \pi/ \, E_{o\lambda} \tag{6}$$

It describes the target reflectance under idealized conditions of illumination (i.e., exo-atmospheric with overhead illumination and the assumption of diffuse reflectance), provides a more intuitive expression of the light levels, and allows instrument properties to be discussed in spectrally independent terms. L_λ is the band-weighted spectral radiance incident on the instrument while observing a target, and $E_{o\lambda}$ is the band-weighted exo-atmospheric solar irradiance at wavelength λ. Using sphere output levels in this range, the calibration is suited for the retrieval of radiances when observing the surface and diffuse skylight, but not the direct sun.

PARABOLA is calibrated once the regression of sphere exitance against PARABOLA radiometer output is determined. The sphere output is placed on a radiometric scale by measurements made with detector standards [Bruegge, et al., 1998b]. In order to achieve the highest radiometric accuracy, two types of laboratory detector standards are used. A QED-200 (made of United Detector Technology inversion layer diodes) is used to measure sphere output for the blue and green spectral bands; and a QED-150 (made of Hamamatsu p-on-n photodiodes) is used for the red and near-infrared channels. Traceability to Système International (SI) units is established through the measurement protocols of current, apertures, and aperture distances.

As these standards are photoconductive devices, they produce a current in response to incident photons. This relationship can be expressed by:

$$i_\lambda=R_\lambda{}^{diode} \, q \, N_\lambda \, . \tag{7}$$

Here $R_\lambda{}^{diode}$ is the photodiode spectral response as a function of wavelength, λ, and is determined as the product of the detector quantum efficiency, filter transmittance, and front surface reflections. Other parameters are i, the device output current, q, the electron charge, and N_λ, the photon rate. Next the energy per photon expression, $E_\lambda=hc/ \, \lambda$, is utilized, with h Planck's constant and c the speed of light. The photon rate is found as the ratio of incident flux, Φ_λ, to photon energy, where

$\Phi_\lambda = L_\lambda A\Omega$, L_λ the incident spectral radiance (independent of the observing sensor) in units of W m^{-2} sr^{-1} μm^{-1}, and $A\Omega$ the photodiode étendue (area times field-of-view product). From these it is determined that the spectral radiance measured by the photodiode is

$$L_d^{diode} = \frac{i \ 1.2395 \ W \ μm \ Amps^{-1}}{A\Omega \ \int S_\lambda^{source} R_\lambda^{diode} \lambda d\lambda}, \tag{8}$$

$$S_\lambda^{source} = L_\lambda^{model} / L_d^{model}. \tag{9}$$

The subscript d is used to denote the photodiode effective center wavelength. The reported radiance are measured at this wavelength. It is determined by a moments analysis of the diode spectral response function. Since there are four laboratory standard configurations, one corresponding to each of the four MISR bands, there are thus four measures of camera-incident radiance, L_d^{diode}. The denominator in Eqn. 8 contains an estimate of the source relative spectral output distribution, λ^{source}. This function is the source spectral radiance, normalized by its value at wavelength d. The limits of integration for the denominator are those of the photodiode response in μm.

To compute the integral required in Eqn. 8, three approaches to the determination of λ^{source} were considered. Ideally, a spectrometer would be used to measure the relative spectral output at each output level (i.e., bulb-on combination). This option was not available. A simple estimate of λ^{source} can be obtained from the spectral Planck blackbody function at a bulb color temperature of 3100 K, normalized by the value of this function at wavelength d. (The temperature value is provided by the sphere vendor). We elected, however, to use a sphere model, rather than a simple blackbody distribution at a single bulb-color temperature. This model comes from integrating sphere theory, and was provided by the vendor.

Let the output of the main sphere, computed as a function of bulb-type, W, be described by:

$$L_\lambda^{main}(W) = \frac{\eta \cdot \Phi(W)}{\sigma \cdot (T(W))^4} \cdot \frac{\rho_\lambda}{1 - \rho_\lambda(1-f)} \cdot \frac{P_\lambda}{\pi A_s} \tag{10}$$

where W refers to the wattage of the bulbs, $\Phi(W) = 30$ or 200 watts and T(W), the filament temperature, is 3100 and 3220 K respectively. The MISR sphere also has a satellite sphere which sits on top of the main sphere. A variable aperture opens or closes to let light from the satellite sphere add to that of the main sphere. The satellite sphere output radiance is described by:

$$L_\lambda^{sat} = \frac{\eta \cdot \Phi(200)}{\sigma \cdot (T(200))^4} \cdot \frac{\rho_\lambda}{1 - \rho_\lambda(1-f)} \cdot \frac{\rho_\lambda \cdot V \cdot P_\lambda}{\pi A_s(1 - \rho_\lambda(1 - f_{sat}))} \quad . \tag{11}$$

Thus, for each of the bulb-on combinations used in the test, n, the total sphere output radiance is given by:

$$L_\lambda^{model}(n) = N(30, n) \cdot L_\lambda^{main}(30) + N(200, n) \cdot L_\lambda^{main}(200) + V_a(n) \cdot L_\lambda^{sat}, \tag{12}$$

where N(W,n) is the number of bulbs turned on at a given level, n, and V_a is the variable aperture of the satellite sphere, a value between 0 and 1.

Other variables in the above equations are:

η = bulb electrical to optical conversion efficiency;

Φ = electrical wattage, either 200W or 30W;

σT^4 = total optical bulb output, integrated over wavelength, $\sigma = 5.67e\text{-}20$ (W μm^{-2} K^{-4});

ρ = sphere reflectance, for Spectraflec, 0.98 for $\lambda < 670$ nm, 0.966 for $\lambda > 865$ nm with a linear fit between these values for 670 nm $< \lambda <$ 865 nm;

f = 0.05, ratio of non-reflecting area of sphere to total sphere area;

P_λ = spectral radiance from sphere, given by Planck's equation;

A_s = sphere surface area, $\pi(1.65m)^2$;

V = view factor of satellite sphere;

$f_{sat} = 0.45$, throughput of satellite sphere.

This model contains an adjustable constant, η, which can be set to one in that only a relative radiance distribution is required. To compute the sphere output radiance at PARABOLA center wavelengths, p, we use the simple formula:

$$L_p^{parabola} = L_p^{model} \bullet L_d^{diode} / L_d^{model} \quad . \tag{13}$$

That is, the energy at a PARABOLA wavelength is proportional to that incident on the photodiode, times a scaling factor that accounts for their wavelength differences. For each PARABOLA channel, the photodiode wavelength closet to the PARABOLA wavelength of interest is used, determined on a channel-by-channel basis.

After both the DN values and PARABOLA-incident radiances are available, the gain coefficients are computed as the result of regressing radiance against DN.

The regression equation used is:

$$DN(n) = G_{0m} + G_{1m} L_p^{parabola}(n) + G_{2m} (L_p^{parabola}(n))^2; \text{ where} \tag{14}$$

G_{im} = monochromatic gain coefficients, i = 0, 1, 2

The incident radiances used in this regression are monochromatic at the computed band centers of the PARABOLA sensors. However, we typically desire band-weighted radiances for the regression equation. Using "L" for monochromatic radiance, "L" for band-weighted radiances and k for the conversion factor, the equation relating these radiances is

$$L^{parabola} = k \, L^{parabola}, \text{ where} \tag{15}$$

$$k = \frac{1}{L_p^{model}} \cdot \frac{\int_{\lambda_l}^{\lambda_u} L_\lambda^{model} \cdot R_\lambda \cdot \lambda \cdot d\lambda}{\int_{\lambda_l}^{\lambda_u} R_\lambda \cdot \lambda \cdot d\lambda} \tag{16}$$

The upper and lower limits on the integration are the endpoints of the PARAOLA response. The conversion to coefficients that are band-weighted are given by using k, defined above:

$$G_0 = G_{0m} \tag{17}$$

$$G_1 = G_{1m} / k$$

$$G_2 = G_{2m} / k^2.$$

Data from PARABOLA were collected on January 23, 1998, in the MISR highbay. The resulting gain coefficients are tabulated in Table 3. Also tabulated is the constant k, which converts from monochromatic to band-weighted PARABOLA radiances.

Table 3. Band-weighted gain coefficients for PARABOLA 23Jan98 calibration

wavelength, nm	k	G_0 (DN)	G_1 (DN / (W m^{-2} μm^{-1} sr^{-1}),	G_2 (DN / (W m^{-2} μm^{-1} sr^{-1})^2)
444	1.0	54.19	3.72	-1.37e-04
551	1.0	4.89	4.11	-2.72e-05
581 (PAR)	1.20	45.13	3.36	-2.00e-05
650	1.0	126.75	5.05	-4.10e-04
860	1.0	40.12	6.32	2.87e-04
944	1.0	-186.52	20.61	-8.79e-04
1028	0.645	-3.71	7.87	1.34e-03
1650	0.999	78.25	9.98	3.74e-02

At best, the calibration described above is good to the MISR calibration requirements of 3% absolute uncertainty (1σ level of confidence). This would be true for PARABOLA wavelengths that are close to the photodiode wavelengths, where the wavelength interpolation scaler is close to unity. The uncertainties at these wavelengths have been documented elsewhere [Bruegge, 1998a]. We would expect larger uncertainties at PARABOLA wavelengths not covered by the standards.The goal of 10% is believed to have been met, based upon a comparison of radiances using data acquired while viewing an integrating sphere at the University of Arizona (UofA), Tucson. At that time the Optical Science Center additionally measured their sphere radiance, using a detector-based standard, portable transfer radiometer.

Although we plan on repeating the PARABOLA radiometric calibration and verification studies, an updated absolute calibration is not considered essential for the retrieval of surface parameters. Rather, methodologies that rely upon reflectance standards are preferred.

4.1 Dark current

By inspection of the radiometric response coefficients, it is observed that the G_0 offset is nonzero. It is important to note that the dark current must be properly accounted for in circumstances where a reflectance standard is used. This technique, where the DN from PARABOLA while observing a target under study is ratioed to that DN when it observes a panel of known reflectance, is common when surface reflectance is desired. Using an dark illumination input of 0.01 equivalent reflectance, the percentage error is computed to be 60%, if the dark current is not first subtracted prior to making the ratio. This is because the dark current is a significant portion of the signal recorded under low-illumination conditions. Even for very bright surfaces the dark current cannot be ignored (the error in doing so is reduced to 1% at an equivalent reflectance of 1).

5. SUMMARY

The PARABOLA III instrument offers higher field-of-view and greater spectral sampling than the original instrument. Its data are particularly suited to retrieving surface BRF, independent of atmospheric conditions. The spectral response functions and fields-of-view have been adequately characterized. Some experience has been gained in determining the radiometric calibration of the instrument. Work continues to extend our certainty of this, and to extend the response determination across the entire dynamic range. Future calibrations will constrain the laboratory regression to the measured offset when there is no incident illumination. It is recommended that reflectance standards be utilized in the retrieval of reflectance parameters. Dark current data acquisitions are also required and should be included in any experimental design.

6. ACKNOWLEDGMENTS

7. REFERENCES

Abdou, Wedad A., Mark C. Helmlinger, James E. Conel, Stu Pilorz, Carol J. Bruegge, Barbara J. Gaitley, and John V. Martonchik, Ground measurements of surface bidirectional reflectance factor (BRF) and hemispherical directional reflectance factor (HDRF) using the portable Apparatus for Rapid Acquisition of Bidirectional observation of the land and atmosphere (PARABOLA III), submitted J. Geophy. Research. (2000).

Bruegge, Carol, Nadine Chrien, and David Haner, A Spectralon BRF data base for MISR calibration applications, accepted to Remote Sens. Environment, 2000.

Bruegge, C.J., N. L. Chrien, R. A. Kahn, J. V. Martonchik, David Diner, Radiometric Uncertainty Tabulations for the Retrieval of MISR Aerosol Products, Conference issue: New Developments and Applications in Optical Radiometry (NEWRAD '97), *Metrologia*, 35, 571-579, 1998a.

Bruegge, C.J., V.G. Duval, N.L. Chrien, R.P. Korechoff, B.J. Gaitley, and E.B. Hochberg, MISR prelaunch instrument calibration and characterization results, IEEE Trans. Geosci. Rem. Sens., Vol. 36, pp. 1186-1198, 1998b.

Chrien,N.L., C.J. Bruegge, Out-of-band spectral correction algorithm for the Multi-angle Imaging SpectroRadiometer, In *Earth Observing System*, Proc. SPIE, Vol. **2820**, Denver, 5-9 August, 1996.

Deering, D.W. and P. Leone, A sphere-scanning radiometer for rapid directional measurements of sky and ground radiance, Remote Sens. of Environ. 19:1- 24, 1986.

Diner, David J., Gregory P. Asner, Roger Davies, Yuri Knyazikhin, Jan-Peter Muller, Anne W. Nolin, Bernard Pinty, Crystal B. Schaaf, and Julienne Stroeve, New directions in Earth Observing: Scientific applications of multi-angle remote sensing, Bull. Am. Meteorol. Soc., 80(11), 2209-2228, November 1999.

Diner, D.J., J.C. Beckert, T.H. Reilly, C.J. Bruegge, J.E. Conel, R. Kahn, J.V. Martonchik, T.P. Ackerman, R. Davies, S.A.W. Gerstl, H.R. Gordon, J-P. Muller, R. Myneni, R.J. Sellers, B. Pinty, and M.M. Verstraete, Multiangle Imaging SpectroRadiometer (MISR) description and experiment overview, IEEE Trans. Geosci. Rem. Sens., Vol. 36, 1072-1087, 1998.

Korechoff, R.P., D. Kirby, E. Hochberg, C. Sepulveda, and V. Jovanovic, Distortion calibration of the MISR linear detectors, in *Earth Observing System*, Proc. SPIE, Vol. **2820**, Denver, 5-9 August 1996.

Lucht, W, Expected retrieval accuracies of bidirectional reflectance and albedo from EOS-MODIS and MISR angular sampling, J. Geophys. Res., 103,8763-8778, 1998.

Martonchik, J.V. (1994). Retrieval of surface directional reflectance properties using ground level multi-angle measurements. Remote Sens. Environ. 50: 303-316.

Martonchik, J.V., D.J. Diner, R. Kahn, T.P. Ackerman, M.M. Verstraete, B. Pinty, and H.R. Gordon, Techniques for the retrieval of aerosol properties over land and ocean using multi-angle imaging, IEEE Trans. Geosci. Rem. Sens., Vol. 36, pp. 1212-1227, 1998.

Wanner, Wolfgang, Expected retrieval accuracies of bidirectional reflectance and albedo from EOS-MODIS and MISR angular sampling, J. Geophys. Res. 1998.

Wehrli, C., Extraterrestrial Solar Spectrum, World Radiation Center (WRC), Davos-Dorf, Switzerland, WRC Publication No. 615, July 1985.